



Switching a pH indicator by a reversible photoacid: A quantitative analysis of a new two-component photochromic system



J. Vallet, J.-C. Micheau, C. Coudret*

Laboratoire des IMRCP, UMR 5623, Université Paul Sabatier (Toulouse III), 118, route de Narbonne, F-31062, Toulouse Cedex 4, France

ARTICLE INFO

Article history:

Received 14 September 2015

Received in revised form

20 October 2015

Accepted 22 October 2015

Available online 30 October 2015

Keywords:

Photochromism

pH photocontrol

Photoacid

Chemical dynamics

Coupled reactions

Spiropyran

ABSTRACT

A UV/visible and pH-metric quantitative analysis of the spirocyanine reversible photoacid **1**-MEH allowed us to determine the pK_a 's of the open and closed forms, the rate constants of relaxation, the quantum yield of decolouration and the UV/visible spectra of the protonated and deprotonated open and closed isomers. The coupling between **1**-MEH and a selected pH-indicator acidochromic dye via proton exchange has also been analysed. The initial pH, stoichiometric ratio between the photoacid and the pH-indicator, light intensity and pK_a range of the pH-indicator have been established to maximize the proton transfer from the photoacid donor to the pH-indicator acidochromic dye acceptor. When the pK_a 's are matched, the two-component system behaves like a single photochromic dye. The proposed model explains why **1**-MEH photo-switches BromoCresol Green but not Methyl-Orange.

© 2015 Elsevier Ltd. All rights reserved.

1. Introduction

Irreversible photoacids such as cationic onium salts [1], triazines [2], arylsulfonyl esters [3] or caged sulfate [4] release a strong acid upon photolysis. They find their main applications as initiators and resists [5]. On the other side, reversible photoacids (such as hydroxypolyaromatics derivatives [6]) exhibit in their excited states, a lower pK_a than in their corresponding ground state. Their reversibility is interesting since the proton accumulation disappears when the light irradiation is switched-off. However, due to their very short lifetimes (from 10⁻⁷ to 10⁻⁹ s), the released protons cannot accumulate in large amount under low power continuous irradiation. In order to favour proton accumulation under low power continuous irradiation, their release must be coupled with a slow isomerisation process. Beside some naphthol derivatives [7], long-lived reversible photo-acids have been designed by modifying already existing photochromic molecules such as 2-hydroxyazobenzenes compounds [8–10]. pK_a photomodulation has also been observed in the spiro-compounds family [11–14]. In polar acidic medium, spirocyanines behave like long-lived reversible photoacids. Accordingly, Liao et al. [15,16]

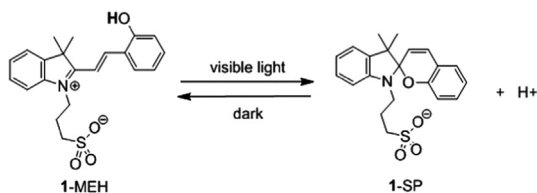
have designed a simple water-soluble spirocyanine merocyanine derivative (Scheme 1).

Because of its easy accessibility, **1**-MEH is now the centre of a growing interest. For instance, it was recently used to switch a water-soluble pH-responsive triethylene glycol monomethyl ether of an hydrazone [17]. This result is particularly appealing since it provides an experimental attempt to couple a reversible photoacid with a pH-responsive equilibrium. Actually, **1**-MEH has been submitted to some physicochemical studies, but only two significant parameters have been obtained namely the quantum yield of photoreaction in DMSO [18] ($\Phi = 0.37$) and the pK_a of **1**-MEH ($pK_a = 7.8$) [14].

In the present paper, we want to show how should be matched the properties of a target proton receiver to those of the **1**-MEH photoacid emitter in order to maximize the extent of photoinduced proton transfer between both partners. In a first part, we have modelled the behaviour of the **1**-MEH photoacid in water. Our approach is based on the proposition of a minimal but realistic global chemical network. Reproduction of all the experimental results in various situations via numerical fittings is then used to confirm the plausibility of the above proposed network. The different parameters obtained (rate constants, equilibrium constants, spectral data) were then used to analyse the optimal conditions to maximize the proton transfer yield from **1**-MEH to an arbitrarily chosen pH-sensitive dye. These theoretical results were

* Corresponding author.

E-mail address: coudret@chimie.ups-tlse.fr (C. Coudret).



Scheme 1. Long-lived reversible 1-MEH photoacid. Protonated merocyanin isomer is labelled “MEH”, while “SP” refers to the deprotonated spiropyran.

then applied to the experimental analysis of the photo-switching of two pH-indicators. As predicted, 1-MEH was found to be able to switch the BromoCresol Green pH-indicator but failed with Methyl-Orange.

2. Determination of the number of pertinent species and establishment of a minimal kinetic network

2.1. Pertinent species

We have monitored the pH variations upon 365 nm irradiation of a non-buffered aqueous solution of 1-MEH and observed that as previously described, the bleaching of the solution (Fig. 1A) was accompanied by a detectable acidification (Fig. 1B). When the photo-steady state (pss) was reached it was found as illustrated on Fig. 1A, that a significant amount of the initial 1-MEH remained, revealing the thermal reversibility of the photoisomerization. It is then expected that the photoconversion at the pss will depend on the 1-MEH initial concentration, the light intensity and the wavelength of irradiation. Fig. 1B shows the relationship between the proton release and the 1-MEH photoconversion. From these data, it appears that the released proton/converted dye ratio is only 0.49. This unexpected result indicates that another species scavenges a part of the released protons. As the decolouration is usually interpreted by the photochemical conversion of the merocyanin into the spiropyran (having a basic indoline nitrogen), we attributed this buffering effect to the building up of the SP form. This thus introduces a new acid-basic couple: 1-SPH/1-SP (see Scheme 2 for the structures).

When the light was turned-off, a colour recovery of the 1-MEH occurred. Fig. 2A displays the corresponding thermal evolution after irradiation. In this particular case, the starting point of the evolution was a high photoconversion photosteady state

(pss) which was reached using non filtered high power white light irradiation. This pss spectrum is thus close to a mixture of the two spiropyranes forms 1-SPH and 1-SP. During the thermal back-reaction in the dark, an isosbestic point (quasi the same as on Fig. 1A) insures that there is no accumulation of any significant absorbing intermediate. This process is globally the reverse to that witnessed under irradiation: there is a gradual decrease of the proton concentration. Interestingly, here also the re-captured protons/recovered dye ratio is around 0.46. Such a value, less than unity, confirms the previous assumption of the coupling between two weak acid systems (1-MEH/1-ME vs 1-SPH/1-SP). Fig. 2B displays the simultaneous curve fitting of four selected wavelengths together with the evolution of the proton concentration during the thermal re-colouration in the dark (*vide infra* and Scheme 2 for the details).

In the same way, the relaxation after KOH addition has been carefully analysed. As shown on Fig. 3, there is an instantaneous appearance of a spectrum likely to be due to the deprotonated isomer 1-ME that decays with time. At the end of the relaxation, residual absorbance at 540 nm indicates the presence of some lasting 1-ME. The size and the shape of this final spectrum depend on the amount of KOH equivalent added. Addition of an excess of HCl restores the initial 1-MEH spectrum. We thus attributed the observed features to the thermal ring-closure of the 1-ME form to the colourless 1-SP one.

As it can be seen on Figs. 1–3, typical monitored transformations last for tens of minutes: it is therefore legitimate to consider that all acido-basic equilibria (involving only proton exchanges with the solution) are always reached during the photochemical transformation. Furthermore, it is known that the isomerization sequence (SP \rightarrow ME) involves several short-lived intermediates [19,20] that could be probed only by ultrafast techniques. Consequently, we have considered that these transients were not kinetically meaningful on the overall used time scale. Similar characteristics can be foreseen for the MEH/SPH processes. An analogous approach was used for the photochemical transformation: the very fast elementary steps were considered to be hidden into an apparent global photochemical process (see Supp. info. part for a short discussion about the assumed fast photochemical processes involving the 1-MEH species as reactant). Therefore the only photochemical process considered is the following 1-MEH + $h\nu \rightarrow$ 1-SP + H^+ , keeping in mind that the equilibrium K_1 : 1-SP + $H^+ =$ 1-SPH is always reached. This

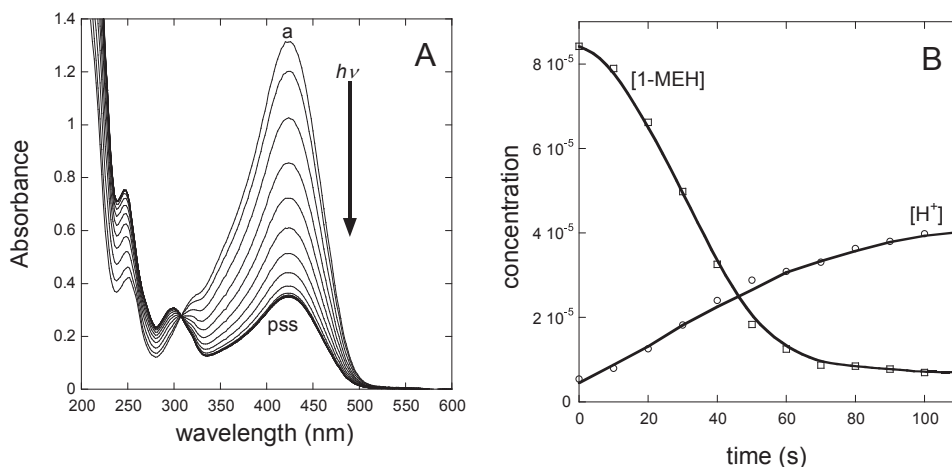
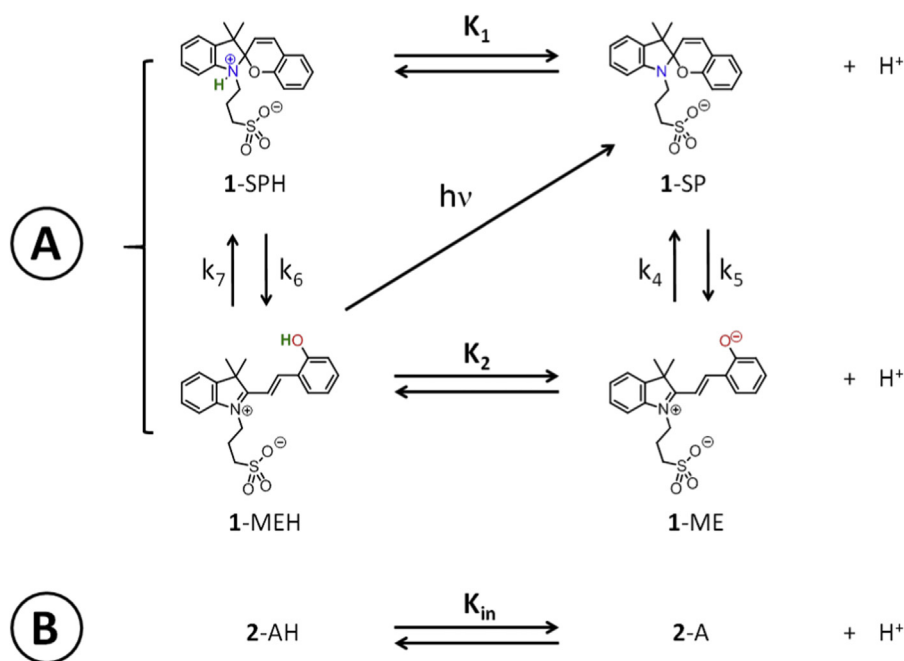


Fig. 1. A: Decolouration of 1-MEH ($8.2 \times 10^{-5} \text{ mol}\cdot\text{L}^{-1}$ in aqueous solution) under 365 nm irradiation; $I_0(365 \text{ nm}) = 2.5 \times 10^{-6} \text{ mol}\cdot\text{L}^{-1}\cdot\text{s}^{-1}$; a: before irradiation; pss: photo-steady state after 500 s of irradiation; ($\Delta t = 30 \text{ s}$). B: Independent experiment showing the simultaneous [1-MEH] and $[H^+]$ monitoring under 436 nm light irradiation in aqueous solution. $I_0(436) = 4.1 \times 10^{-6} \text{ mol}\cdot\text{L}^{-1}\cdot\text{s}^{-1}$, $\text{pH}(\text{initial}) = 5.3$; $\text{pH}(\text{pss}) = 4.39$. Continuous lines are from the numerical fitting by the model (see below and supp. info. part).



Scheme 2. Global kinetic scheme used in this work: A: Structural changes of the reversible photoacid **1-MEH** with or without irradiation with visible light. B: independent pH-sensitive equilibrium of an acidochromic dye. Networks A and B are merged for proton transfer experiments.

apparent photochemical transformation is also the one that has been assayed directly on Fig. 1. Indeed this figure allows also a rough graphic estimation of the quantum yield of **1-MEH** photo-decoloration. Thus from the slope of the decay, $\Phi \approx \Delta[1\text{-MEH}]/\Delta^*I_0 \approx 0.36$ (i.e. close to 0.38 ± 0.03 : the value found from the curve fitting, *vide infra*).

The simplest global kinetic network that takes into account all these experimental observations is thus the following (Scheme 2A).

2.2. Analysis of the kinetic network

Using homemade software, the consistency of the above proposed network was assayed by fitting a set of independent experimental kinetics. Results of such fits are displayed as solid lines in Fig. 2B and in Fig. 3S in *supp. info. part*. A stable set of parameters has been extracted, namely the relaxation rate constants k_i , pK_a

values of the open and closed forms and the quantum yield of decoloration as defined above (Table 1). This calculation also helped us to confirm the molar extinction coefficients of the species from which the whole spectra of the four species have been recalculated (Fig. 4).

Contrarily to the initial report, the **1-SPH** form is not a strong acid as a $pK_a \approx 4.3$ was determined. Upon irradiation, the appearance of the closed form (**1-SPH**), more acidic by ≈ 3.5 units than the initial **1-MEH** dye, and the change of composition of the mixture explain the photoacid behaviour. Speciation diagrams in the dark and at the pss are displayed on Fig. 4S in the *Supplementary information part*. Results show that the reversibility of the **1-MEH** photoacid is not solely due to the ring-opening of the protonated forms (**1-SPH** \rightarrow **1-MEH** (k_6)) but also to an exchange between the open and closed deprotonated isomers (**1-SP** \leftarrow **1-ME** (k_4 ; k_5)). Any attempt to remove one parameter or to fix

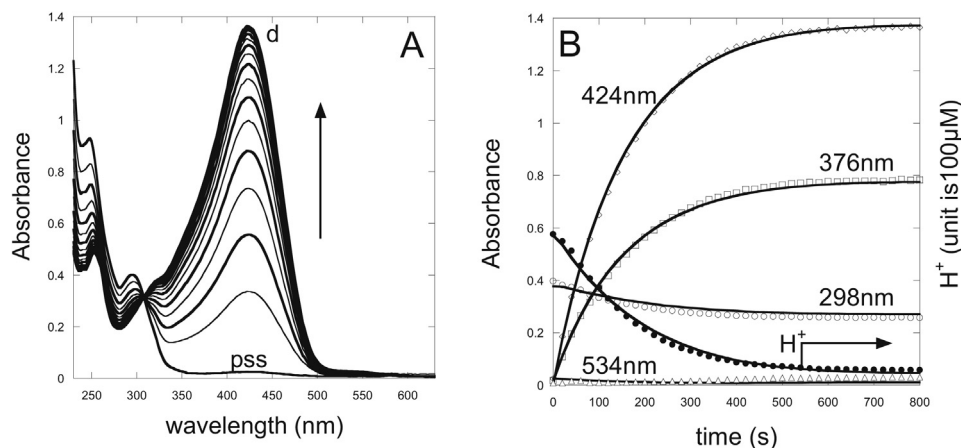


Fig. 2. A: Spectral evolution ($\Delta t = 20$ s) of **1-MEH** (8.5×10^{-5} mol.L $^{-1}$ in aqueous solution) during the thermal relaxation after white light irradiation; pss: photo-steady state; d: equilibrium state in the dark. B: Absorbances and $[\text{H}^+]$ monitoring (pH from 4.22 to 5.40) during the thermal relaxation. Continuous lines are from the numerical fitting of the model shown on Scheme 2 (part A).

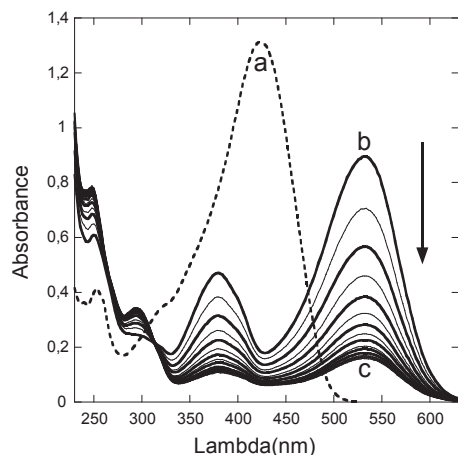


Fig. 3. A: Spectral evolution ($\Delta t = 10$ s) of **1-MEH** (8.1×10^{-5} mol.L $^{-1}$ in aqueous solution) after addition of 1 equivalent of strong base ($[\text{OH}^-]_0 = 8.1 \times 10^{-5}$ mol.L $^{-1}$). Note the appearance of the transient spectrum at 534 and 376 nm a: before base addition or after HCl acidification; b: just after base addition; c: basic equilibrium.

Table 1

Optimized thermodynamic and kinetic parameters values obtained after numerical fitting.

Parameters	Value
$\text{pK}_a(\mathbf{1-MEH}/\mathbf{1-ME})$	7.75 ± 0.3
$\text{pK}_a(\mathbf{1-SPH}/\mathbf{1-SP})$	4.3 ± 0.3
k_4	$(3 \pm 0.7) \times 10^{-2} \text{ s}^{-1}$
k_5	$4.6 \times 10^{-3} \text{ s}^{-1}$
k_6	$8 \times 10^{-3} \text{ s}^{-1}$
k_7	0
$\text{Phi} (h\nu)$	0.38 ± 0.03

it at a different value resulted in a systematic loss of the fitting accuracy. While more detailed since several new parameters have been determined, there are no fundamental discrepancies between our modelling approach and the second-order treatment by Johns et al. [18]. For instance, our first order relaxation rate constant $\mathbf{1-SP} \rightarrow \mathbf{1-ME}$ ($k_5 = 4.6 \times 10^{-3} \text{ s}^{-1}$) is of the same order of magnitude than the apparent pseudo first-order rate constant that can be calculated in their $7.03 \times 10^{-5} \text{ M}$ aqueous solution: $73 \text{ s}^{-1} \text{ M}^{-1} \times 7.03 \times 10^{-5} \text{ M} = 5.13 \times 10^{-3} \text{ s}^{-1} \approx 4.6 \times 10^{-3} \text{ s}^{-1}$

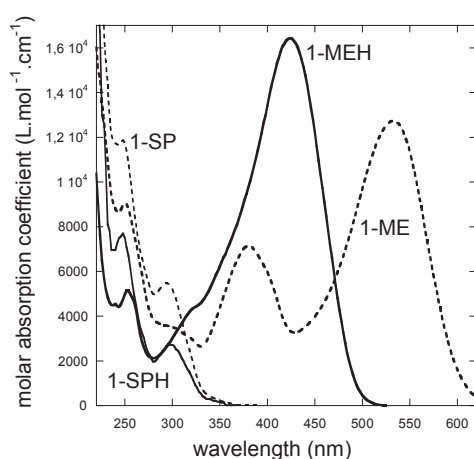


Fig. 4. Re-calculated UV/visible spectra of the four species involved in the **1-MEH** reversible photoacid system (see Table 1S in the supp. info. part).

Open forms absorptions spectra are dominated by a low energy, protonation sensitive band that shifts from 540 nm up to 420 nm for respectively **1-ME** and **1-MEH**. On the other hand, spiropyrane closed forms exhibit an absorption band around 300 nm, the deprotonated form **1-SP** being more intense than the **1-SPH** acid. Remarkably, their maxima are poorly affected by protonation: this can be interpreted by the lack of any substitution on the indoline moiety. This also is in agreement with the observed isosbestic points in Figs. 1 and 2. All the compounds absorb at 260 nm, the deprotonated forms (**1-SP** and **1-ME**) being the strongest.

3. Modelling of the coupling between **1-MEH** and a pH-indicator acidochromic dye

With the parameters in hand, we used kinetic numerical modelling to analyse “*in silico*” the coupling between the **1-MEH** photoacid and a pH-indicator **2-AH** according to the complete (A + B) kinetic network from Scheme 2.

3.1. Determination of the optimal pK_a range

Several constraints were examined: the pK_a values of the pH indicator **2-AH** (pK_{ind}), the initial pH, the stoichiometric ratio **1-MEH/2-AH** and the light intensity. Such a situation involving the coupling of several thermal and photochemical equilibria under non-equilibrium conditions (*i.e.* at the photosteady state) has been managed thanks to the numerical integration of a nonlinear differential equations system including 9 species and 12 pseudo-elementary processes (see Supp. info. part). Fig. 5A compares the pH drop responses upon irradiation of the free **1-MEH** with mixtures of **1-MEH** plus 40% mole/mole of a pH indicator acidochromic dye exhibiting a pK_{ind} value at either, 3, 6 or 9. When the pK_{ind} of the pH-indicator **2-AH** is too high or too low the pH drop is unaffected by the presence of the additive. However, with a pH indicator exhibiting a pK_{ind} at 6, the pH drop is quenched: the released protons are partly absorbed by the basic form of the pH-indicator. This can be also analysed by examining the % switching of the pH-indicator acidochromic dye (*i.e.* the yield of the proton transfer). As previously discussed, the coupling readily vanishes for pK_{ind} values 3 and 9 (Fig. 5B) and is maximal for pK_{ind} values close to 6 (in between the pK_a 's of the closed (4.3) and open (7.75) photoacid isomers): the irradiation of **1-MEH** induces the switching, albeit non quantitative, of the pH-indicator additive. Practically, the two-component system behaves then like a single new photochromic dye. An empirical approach leading to the same conclusion was recently proposed by Chen et al. [24]. However, looking carefully at Fig. 4B, it can be seen that the optimal initial pH does not occur systematically at the expected $\text{pH} = \text{pK}_{\text{ind}}$. For instance, for $\text{pK}_{\text{ind}} = 3$ the optimal pH is around 5.5, for $\text{pK}_{\text{ind}} = 6$ at 6.5 and at 7.5 for $\text{pK}_{\text{ind}} = 9$.

3.2. Influence of the light intensity on the yield of proton transfer

The efficiency of the proton transfer from the photoacid to a pH-indicator acidochromic dye has been also investigated by varying simultaneously the stoichiometric ratio and the light intensity. The efficiency has been regarded either as a chemical yield (% of switched pH-indicator) or as a protonation quantum yield (rate of pH-indicator protonation vs absorbed light intensity by the photoacid). Fig. 6A shows that the % of switched pH-indicator is higher at low pH-indicator loading ($[\text{pH-indicator}]/[\mathbf{1-MEH}]$ stoichiometric ratio). The levels-off at high intensity is related to the limited amount of protons which can be released by the photoacid ($[\text{H}^+] \text{ released max} < [\mathbf{1-MEH}]_0$). When the light intensity is decreased, the thermal proton re-capture becomes significant and limits the %

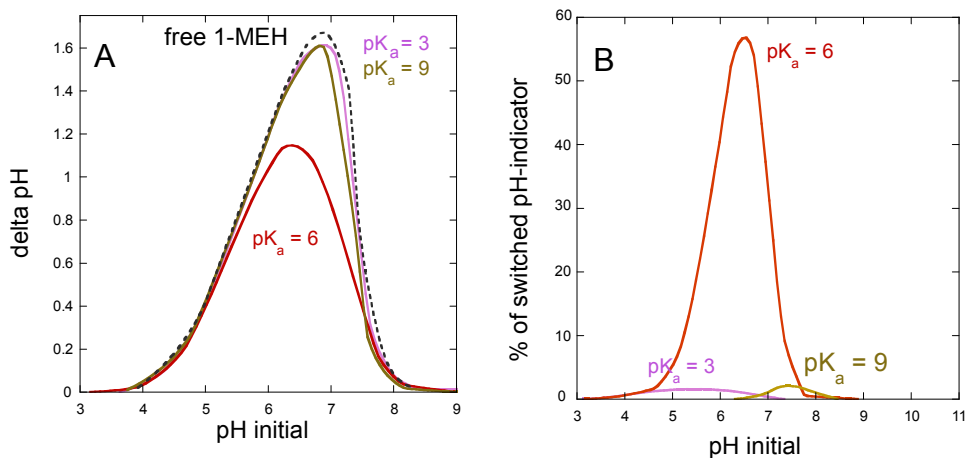


Fig. 5. A: Numerical simulation of the pH drop upon irradiation until pss ($I_0 = 1.46 \times 10^{-6} \text{ mol L}^{-1} \cdot \text{s}^{-1}$). Dashed curve, free 1-MEH: $3.5 \times 10^{-5} \text{ M}$ in water; curve $pK_a = 3$: 1-MEH $3.5 \times 10^{-5} \text{ M}$ with $1.5 \times 10^{-5} \text{ M}$ of a pH-indicator AH exhibiting a pK_a at 3; curve $pK_a = 6$: same with AH ($pK_a = 6$). Curve $pK_a = 9$: with AH ($pK_a = 9$). B: % of switched pH-indicator ($([AH]_{\text{pss}} - [AH]_{\text{initial}}) / [AH]_0$) upon irradiation. Note the buffering of the pH drop (A) and the significant switching effect (B) when the pK_a of the added pH indicator is around 6.

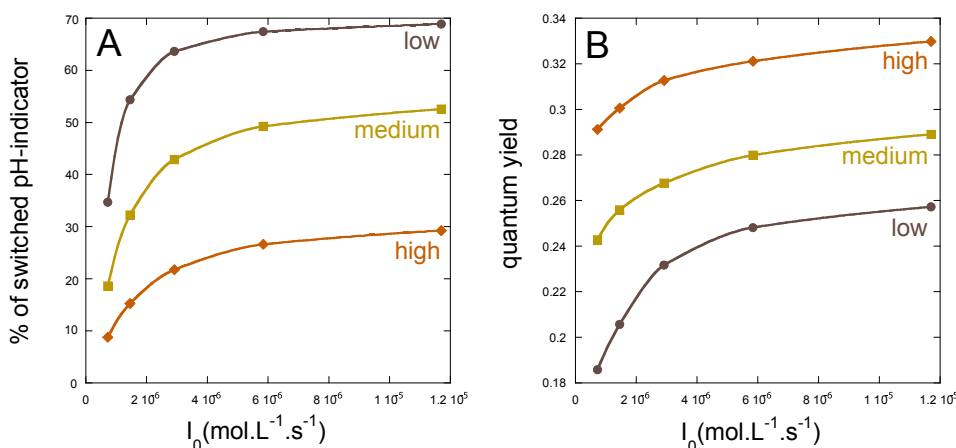


Fig. 6. A: Variation of the % of switched pH-indicator ($pK_a = 6$) upon irradiation of 1-MEH ($3.5 \times 10^{-5} \text{ M}$ in water solution) at various light intensities (pH initial = 6.71). Note the better switching at low pH-indicator loading. B: Quantum yield of proton capture by the pH-indicator dye. Note the drop of the quantum at low intensity. pH-indicator loading = $[pH\text{-indicator}] / [1\text{-MEH}]$; low: 0.43; medium: 0.83; high: 1.67.

of switched pH-indicator. On the other hand, Fig. 6B displays the quantum yield of proton capture by the pH-indicator. As expected, the situation is reversed, results show that for the highest loading and the highest light intensity, the quantum yield of proton capture reaches 0.33 *i.e.* a value close to the quantum yield of photoacid isomerization (0.37) since in these conditions proton re-capture within the photoacid manifold is negligible. On the contrary, at the lowest light intensities, thermal relaxation of the photoacid becomes significant and as a consequence proton release is limited: the quantum yield of proton capture vanishes. This decrease is more apparent at low loading.

These simulations show that the interplay between all processes impedes a complete conversion of the pH indicator.

4. Experimental photoswitching of a pH-indicator acidochromic dye by 1-MEH

To illustrate the previous study, we have checked experimentally the pH switching capabilities of the 1-MEH spiropyrane photoacid in presence of pH indicators with variable pK_a 's. For this purpose, two pH indicators, namely methyl orange (MO) [21] and bromocresol green (BCG) have been selected. The ordering of the

pK_a s is the following: $pK_{\text{ind}}(\text{MO}) = 3.39 < pK_a(1\text{-SPH}) = 4.3 < pK_{\text{ind}}(\text{BCG}) = 4.83 < pK_a(1\text{-MEH}) = 7.75$. As expected from Fig. 5B, preliminary experiments have confirmed that the % of switched MO was limited (less than 0.3%) while, on the contrary, % of switched BCG reached more than 40%. Therefore, most of the experimental work has been carried-out with BCG. This pH-indicator exhibits an absorption band centred at 614 nm associated with the deprotonated form (BCG) and a band centred at 444 nm associated with the protonated form (BCGH) (see [supp. info. part](#)).

Fig. 7A shows the switching of BCG during irradiation of 1-MEH. The decrease at 616 nm is mainly related to the protonation of BCG while the decrease at 420 nm mostly corresponds to the photo-induced ring closure of the 1-MEH photoacid. Without changing the extracted values of model parameters but putting the pK_a of the pH-indicator at its BCG value ($pK_{\text{ind}} = 4.8$), allowed us to reproduce the spectral evolution (Fig. 7B) using the molar extinction coefficients of the various species. This result is particularly interesting since it confirms the predictability of the proposed model when the 1-MEH long-lived reversible photoacid is put in a working condition *i.e.* to switch an acidochromic dye. The success of the fitting of this independent experiment is a strong indication that

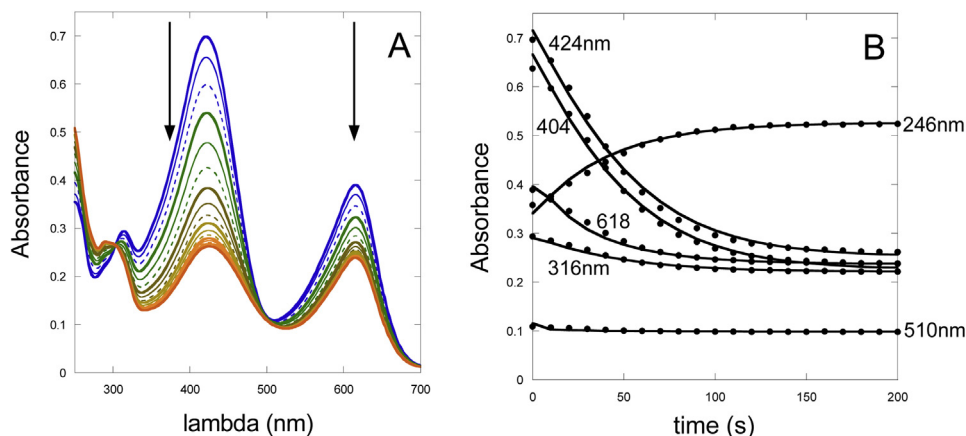


Fig. 7. A: Spectral evolution of a BCG + 1-MEH mixture ($[BCG]_0 = 1.31 \times 10^{-5}$; $[1-MEH]_0 = 2.9 \times 10^{-5}$ mol L $^{-1}$ (BCG loading ratio = 0.45) under 405 nm irradiation ($I_0 = 3.6 \times 10^{-7}$ mol L $^{-1}$.s $^{-1}$); arrows indicate the direction of evolution ($\Delta t = 10$ s). pH initial was around 5.2; B: Evolution of the absorbances at 6 selected wavelengths. Continuous lines: numerical simulation using the proposed model with all the extracted parameters (pK_a 's, rate constants and molar extinction coefficients).

the main features of the photoacid mechanism of proton release have been interpreted. The model confirms that the pH variation has crossed the BCG pK_a value and has switched the $[BCGH]/[BCG]$ ratio. Moreover the model was able to simulate accurately the evolution of the concentrations of the various species either under irradiation or during the thermal relaxation in the dark (see [supp. info part](#)).

5. Summary

The reversible photoacid behaviour of the water soluble, negative photochromic dye 1-MEH has been investigated. Although apparently trivial, the presence of simultaneous acido-basic and isomerization processes renders the global dynamic behaviour barely predictable, especially in quantitative terms. However some reliable trends could be extracted thanks to numerical analysis. In particular, the importance of the weakly basic 1-SP form as well as of the initial pH has been stressed out in the H $^+$ production. As this dye is expected to be a useful component to photo-trigger pH controlled phenomena in a similar way to related examples [22,23], we have also defined the optimal operating conditions to maximize the observed effect, using a pH-indicator dye as H $^+$ receptor. Not only the receptor's pK_a must fall in a limited window conditioned by the photoacid itself, but initial pH is also of importance to ensure maximum proton transfer between both components. This is a typical situation of coupled chemical reactions Thus the 1-MEH photoacid can effectively be used to photoswitch efficiently a pH-indicator dye whose pK_a lies in the 4–6 range. Our results provide some theoretical guidelines to the question of the optimal use of long-lived photoacids for light controlled pH-drop and actuations [24]. For instance, artificial molecule-releasing devices [25–27] could be designed from long-lived reversible photoacids in order that the effect of a drug will depends on the conditions where this drug is released and re-captured.

Acknowledgements

CNRS and University Toulouse III - Paul Sabatier are acknowledged for financial support.

Appendix A. Supplementary data

Supplementary data related to this article can be found at <http://dx.doi.org/10.1016/j.dyepig.2015.10.025>.

References

- [1] Crivello JV. *J Polym Sci Part A Polym Chem* 1999;37:4241–54.
- [2] Pohlers G, Scaiano JC, Sinta R. *Chem Mater* 1997;9:3222–30.
- [3] Klan P, Solomek T, Bochet CG, Blanc A, Givens R, Rubina M, et al. *Chem Rev* 2013;113:119–91.
- [4] Barth A, Corrie JET. *Biophys J* 2002;83:2864–71.
- [5] Ling J, Naren G, Kelly J, David B, Fox DB, de Silva AP. *Chem Sci* 2015;6:4472–8.
- [6] a Hizuka H. *Acc Chem Res* 1985;18:141–214.
b Marciniak B, Kozubek H, Paszyc S. *J Chem Educ* 1992;69:247–9.
- [7] Nunes RMD, Pineiro M, Arnaut LG. *J Am Chem Soc* 2009;131:9456–62.
- [8] Emond M, Le Saux T, Maurin S, Baudin JB, Plasson R, Jullien L. *Chem Eur J* 2010;16:8822–31.
- [9] Emond M, Sun J, Grégoire J, Maurin S, Tribet C, Jullien L. *Phys Chem Chem Phys* 2011;13:6493–9.
- [10] Le Saux T, Plasson R, Jullien L. *Chem Commun* 2014;50:6189–95.
- [11] Zhou J, Li Y, Tang Y, Zhao F, Song X, Li E. *J Photochem Photobiol A Chem* 1995;90:117–23.
- [12] Sumaru K, Takagi T, Satoh T, Kanamori T. *J Photochem Photobiol A Chem* 2013;261:46–52.
- [13] Ziolkowski B, Florea L, Theobald J, Benito-Lopez F, Diamond D. *Soft Matter* 2013;9:8754–60.
- [14] Abeyrathna N, Liao Y. *J Am Chem Soc* 2015;137:11282–4.
- [15] Shi Z, Peng P, Strohecker D, Liao Y. *J Am Chem Soc* 2011;133:14699–703.
- [16] Luo Y, Wang C, Peng P, Hossain M, Jiang T, Fu W, et al. *J Mater Chem B* 2013;1:997–1001.
- [17] Tatum LA, Foy JT, Aprahamian I. *J Am Chem Soc* 2014;136:17438–41.
- [18] Johns VK, Wang Z, Li X, Liao Y. *J Phys Chem A* 2013;117:13101–4.
- [19] Deniel MH, Lavabre D, Micheau JC. In: Crano JC, Guglielmetti RG, editors. *Organic photochromic and thermochromic compounds, vol. 2*. New York: Kluwer Academic, Plenum Press; 1999. p. 167.
- [20] Markworth PB, Adamson BD, Coughlan NJA, Goerigk L, Bieske EJ. *Phys Chem Chem Phys* 2015;17:25676–88.
- [21] Boily JF, Seward TM. *J Soln Chem* 2005;34:1387–406.
- [22] Raymo FM, Giordani S. *Org Lett* 2001;3:3475–8.
- [23] a Silvi S, Constable EC, Housecroft CE, Beves JE, Dunphy EL, Tomasulo M, et al. *Chem Eur J* 2009;15:178–85.
b Silvi S, Constable EC, Housecroft CE, Beves JE, Dunphy EL, Tomasulo M, et al. *Chem Commun* 2009:1484–6.
- [24] Chen H, Liao Y. *J Photochem Photobiol A Chem* 2015;300:22–6.
- [25] Johns VK, Patel PK, Hassett S, Calvo-Marzal P, Qin Y, Chumbimuni-Torres KY. *Anal Chem* 2014;86:6184–7.
- [26] Guardado-Alvarez TM, Russell MM, Zink JL. *Chem Commun* 2014;50:8388–90.
- [27] Wang Z, Johns VK, Liao Y. *Chem Eur J* 2014;20:14637–40.